Perspectives for the microbial production of methyl propionate integrated with product recovery

Pereira, Joana P.C.; van der Wielen, Luuk A.M.; Straathof, Adrie J.J.

DOI
10.1016/j.biortech.2018.01.118

Publication date
2018

Document Version
Accepted author manuscript

Published in
Bioresource Technology

Citation (APA)
Pereira, J. P. C., van der Wielen, L. A. M., & Straathof, A. J. J. (2018). Perspectives for the microbial production of methyl propionate integrated with product recovery. *Bioresource Technology*, *256*, 187-194. https://doi.org/10.1016/j.biortech.2018.01.118

Perspectives for the microbial production of methyl propionate integrated with product recovery

Joana P. C. Pereira

Luuk A. M. van der Wielen

Adrie J. J. Straathof*

Department of Biotechnology, Delft University of Technology, van der Maasweg 9, 2629HZ Delft, the Netherlands

***Correspondence**: Adrie J. J. Straathof, Department of Biotechnology, Delft University of Technology, van der Maasweg 9, 2629HZ Delft, the Netherlands

E-mail: A.J.J.Straathof@tudelft.nl

Telephone: +31152782330

Abstract

A new approach was studied for bio-based production of methyl propionate, a precursor of methyl methacrylate. Recombinant *E. coli* cells were used to perform a cascade reaction in which 2-butanol is reduced to butanone using alcohol dehydrogenase, and butanone is oxidized to methyl propionate and ethyl acetate using a Baeyer-Villiger monooxygenase (BVMO). Product was removed by *in-situ* stripping. The conversion was in line with a model comprising product formation and stripping kinetics. The maximum conversion rates were 1.14 g-butanone/(L h), 0.11 g-ethyl acetate/(L h), and 0.09 g-methyl propionate/(L h). The enzyme regioselectivity towards methyl propionate

was 43% of total ester. Starting from biomass-based production of 2-butanol, full-scale ester production with conventional product purification was calculated to be competitive with petrochemical production if the monooxygenase activity and regioselectivity are enhanced, and the costs of bio-based 2-butanol are minimized.

Keywords: Biomaterials; bioprocess engineering; integrated product recovery; modeling

1. Introduction

Polymethyl methacrylate (PMMA) is a valuable thermoplastic known for its excellent performance characteristics, and its vast application in several fields (Ali et al., 2015). Its market size is expected to exceed USD 11 billion by 2022 (Global Market Insights, 2016). Nonetheless, industrial production methods rely on fossil carbon sources and precious metal catalysts, and generate greenhouse gases (Clegg et al., 1999; Liu et al., 2006). To mitigate these issues, the producers seek opportunities for biomass-based approaches for methyl methacrylate production.

In the present work, we propose a pathway for biomass-based methyl methacrylate that comprises a series of reactions under distinct oxygen regimes, which is summarized in Fig. 1. First, fermentable sugars such as lignocellulosic hydrolysate are converted into butanone by anaerobic fermentation (Chen et al., 2015; Yoneda et al., 2014). This fermentation includes butanone conversion into 2-butanol by a suitable NADH-dependent alcohol dehydrogenase (ADH), to generate the essential NAD^+ required for closing the redox balance. The conditions for profitable bio-based 2-butanol production have been determined (Pereira et al., 2017). Next, in an aerobic biotransformation, 2-butanol is oxidized back to butanone by a $NADP^+$-dependent ADH, and butanone is further oxidized by O_2 using cyclohexanone monooxygenase (CHMO). CHMO inserts one oxygen atom in butanone, while the other atom is reduced with NADPH to water. Although oxygen insertion next to the most substituted carbon yields the so-called normal product, ethyl acetate, the regioselectivity of this reaction has been shifted to the abnormal product, methyl propionate (van Beek et al., 2017). Methyl propionate is finally condensed with formaldehyde to form methyl methacrylate, in a downstream

chemistry step which is outside the scope of this study, as it resembles the last part of the existing Alpha process for methyl methacrylate production (Eastham et al., 2015). The current research evaluates an integrated biotransformation for methyl propionate production, aiming to identify the major process bottlenecks at an early stage of strain engineering and process design. Recombinant *Escherichia coli* cells expressing two distinct fused redox-complementary enzymes (Aalbers and Fraaije, 2017) have been used to determine the conversion rate of 2-butanol and identify the rate-limiting step in the cascade reaction.

As this is a strictly aerobic conversion, the continuous aeration promotes the stripping of the volatile biotransformation products along with the exhaust gas. Although stripping is useful to alleviate product toxicity and enhance product recovery costs (de Vrije et al., 2013; Xue et al., 2013), uncontrolled product loss makes the ester quantification a challenging task, demanding full understanding of the stripping process. Using stripping and product formation kinetics, the performance of a conceptual 120 kton/a process for bio-based methyl propionate production will be assessed.

The inevitable by-product, ethyl acetate, is an environmentally friendly solvent with broad application range, and its commercial value is close to that of methyl propionate itself (Straathof and Bampouli, 2017). Despite its current petrochemical-based production, numerous yeast species are natural ethyl acetate producers, particularly *Kluyveromyces marxianus* with an outstanding formation rate of 0.67 g/g/h, and 56% of the maximum theoretical yield (Urit et al., 2013). Recently, Kruis et al. (2017) reported ethyl acetate production using recombinant *E. coli*, reaching 33% of the maximum theoretical yield. In the two-step process proposed herein, the maximum achievable theoretical yield is 0.453 $g_{ester}/g_{glucose}$, similar to that of direct glucose conversion (Löser

et al., 2014). This suggests the high potential of the proposed process for bio-based ester production.

2. Material and Methods

2.1. Bacterial strains and culture media

Fusion constructs containing the cyclohexanone monooxygenase (TmCHMO) gene from *Thermocrispum municipale*, and either the alcohol dehydrogenase TbADH obtained from *Thermoanaerobacter brockii*, or the MiADH obtained from *Mesotoga infera*, have been developed by Aalbers and Fraaije (2017). *E. coli* NEB® 10-beta cells (New England Biolabs), harboring the plasmids which contained the gene fusions, were kindly provided by the Molecular Enzymology Group, Groningen Biomolecular Sciences and Biotechnology Institute.

Recombinant cells from -80°C glycerol stocks were used in the experiments. Pre-cultures were first grown overnight at 37°C and 200 rpm, in 15 mL Luria Broth (LB) medium containing 10.4 g/L tryptone peptone, 10.4 g/L sodium chloride, 4.8 g/L yeast extract, and 50 mg/L ampicillin.

Terrific Broth (TB) contained 12.0 g/L tryptone peptone, 24.0 g/L yeast extract, 5.0 g/L glycerol, 2.4 g/L KH_2PO_4, 12.5 g/L K_2HPO_4, and 50 mg/L ampicillin. Minimal Medium (MM) contained 3.0 g/L KH_2PO_4, 7.3 g/L K_2HPO_4, 2.0 g/L NH_4Cl, 5.0 g/L $(NH_4)_2SO_4$, 8.4 g/L MOPS, 0.5 g/L NaCl, 0.5 g/L $MgSO_4 \cdot 7H_2O$, 4.0 g/L glucose$\cdot H_2O$, and 1 mL/L trace element solution. The trace element solution contained 3.6 g/L $FeCl_2 \cdot 4H_2O$, 5.0 g/L $CaCl_2 \cdot 2H_2O$, 1.3 g/L $MnCl_2 \cdot 2H_2O$, 0.4 g/L $CuCl_2 \cdot 2H_2O$, 0.5 g/L $CoCl_2 \cdot 6H_2O$, 0.9 g/L $ZnCl_2$, 0.03 g/L H_3BO_4, 20.0 g/L $Na_2EDTA \cdot 2H_2O$, 0.1 g/L $Na_2MoO_4 \cdot 2H_2O$, and

1.0 g/L thiamine HCl. The media were supplemented with 50 mg/L ampicillin and 40 mg/L L-leucine, and the final pH was adjusted to 7 using 1 mol/L K_2HPO_4.

2.2. Methyl propionate formation in shake flasks

The pre-cultures were used to inoculate 50 mL of MM or TB medium (1% v/v) in 2 L polycarbonate baffled flasks with vent cap (Thermo Fisher), and these were incubated at 24°C and 200 rpm. When the optical density at 600 nm (OD_{600}) reached 0.5, L-arabinose and 2-butanol (Sigma-Aldrich, the Netherlands), were added to final concentrations of 0.2 g/L and 0.75 g/L, respectively. Samples for metabolite analysis were taken immediately, 24 h, and 40 h after induction. The samples were centrifuged at 4000 g for 10 min, and both supernatant and cell pellet were stored at -20°C until further analysis. The experiments were performed in duplicate.

2.3. Ester formation integrated with product recovery

2.3.1. Preliminary gas stripping studies

To characterize the *in-situ* removal of biotransformation products by gas stripping, model solutions were prepared using accurately weighed amounts of demi-water, 2-butanol, butanone, methyl propionate, and ethyl acetate (Sigma-Aldrich, the Netherlands).

Before each experiment, the glassware was cleaned with water and soap, dried overnight at 70°C, and accurately weighed at room temperature. A 3.0 L Biostat fermentor (Applikon, the Netherlands), fitted with typical sensors for dissolved oxygen, temperature, pressure, and pH, was used with a working volume of 1.0 L. The reactor was operated at 24.0±0.5°C, 500 rpm, and the air flow was varied between 1–2.5 vessel

volumes per minute (vvm). The off-gas port of the reactor was attached to the condensation system (Fig. 2), which comprised an Erlenmeyer containing 128 g of butyl acetate in an ice bath, and a series of two 50 cm Graham-type condensers connected to 250 mL Erlenmeyer flasks, submerged in the cryostat at -7 °C (ECO RE 620, Lauda). Before being released to the atmosphere, the stripped vapor was additionally bubbled in 150 mL of chilled water in an ice bath.

The system was monitored using MFCS/win 3.0 software (Sartorius), and aqueous samples were collected hourly for GC analysis. Upon termination of the experiment, the volume, mass and composition of the media and condensates were determined. The experiments were performed in duplicate.

2.3.2. Biotransformation integrated with *in-situ* stripping and absorption

Ester biotransformation integrated with *in-situ* stripping and absorption was performed using the experimental set-up described in Fig. 2, under aseptic conditions. The reactor was operated at 24.0±0.5°C and 500 rpm, the air flow was 1 vvm, and the pH was controlled at 7.0±0.2 using either KOH (4 mol/L) or H_2SO_4 (0.5 mol/L). Pre-cultures were used to inoculate 1.0 L working volume of sterile TB or MM (10% v/v), supplemented with glycerol or glucose, respectively, to obtain 40 g/L of these carbon sources. Once the OD_{600} reached ~0.5, L-arabinose and 2-butanol were added. Samples from the bulk were collected hourly for metabolite analysis.

2.4. Analytical Methods

Cell growth was monitored by measuring the OD_{600} in a spectrophotometer (Biochrom Libra Instruments, Netherlands), and correlated to cell dry weight (CDW). CDW was

determined by centrifuging 2 mL aliquots of several dilutions of broth in pre-weighed Eppendorf at 4000 g for 10 min, and drying the cell pellets at 70°C for 48 h before weighing.

To assess protein expression, cells grown in each medium were lysed using BugBuster Plus Lysonase™ solution (Novagen®). The cell pellet fraction was resuspended in 200 µL of KH_2PO_4 buffer (pH 7.5). Both supernatant and cell pellet fractions were loaded onto an SDS-PAGE gel (GenScript, Benelux), and analyzed according to the recommendations of the gel supplier.

Cell maintenance requirements were estimated from glucose consumption by non-growing cells during stationary phase. Glucose was quantified colorimetrically using the Megazyme Glucose Determination Reagent (Megazyme International Ireland). Glycerol was quantified by HPLC (Waters, USA), using an Aminex BioRad HPX-87Hf column (300 x 7.8 mm, particle size 9 µm) at 60°C, with phosphoric acid (147 mg/L) as eluent.

Aqueous concentrations of volatiles were determined via GC (InterScience, the Netherlands), using a Zebron™ ZB-WAX-PLUS column (30 m x 0.32 mm x 0.50 µm). 1-Pentanol (320 mg/L) was used as internal standard. The temperature was 30°C for 5 min, followed by a gradient of 20°C/min for 5 min. The temperatures of the injector and FI detector were 200°C and 250°C, respectively.

Vapor concentrations of volatiles were determined via Compact GC 4.0 (InterScience, the Netherlands), using a Rtx®-1 column (30 m x 0.32 mm x 5.0 µm), with an isothermal program at 45°C for 14 min. For the low concentration range, an additional thermal desorption (TD) system, composed of a sorbent tube with Tenax® TA and a focusing trap U-T2GPH-2S, was used to concentrate the products.

2.5. Modeling studies

2.5.1. Integrated biotransformation and stripping of methyl propionate

The biotransformation model aims to describe the system where 2-butanol, butanone, ethyl acetate, methyl propionate, water, and O_2 are consumed/formed and stripped at specific rates. We consider batch mode with non-growing cells, but the equations can be modified to describe abiotic or continuous processes. Homogeneous vapor and liquid phases were assumed. The stripping of volatile biotransformation products has been modeled as a two-step process describing product transfer from the liquid to the vapor phase, followed by discharge via the off-gas (cf. Löser et al. (2005) and Urit et al.(2011)). The molar concentrations $C_{i,L}$ of each component i in the liquid phase, and respective molar fractions x_i, are:

$$C_{i,L} = \frac{n_{i,L}}{V_L} \quad (1)$$

$$x_i = \frac{n_{i,L}}{\sum n_{i,L}} \quad (2)$$

Analogously, the molar fractions in the vapor phase y_i are equal to:

$$y_i = \frac{n_{i,G}}{\sum n_{i,G}} \quad (3)$$

The following reactions are considered, assuming that cellular redox homeostasis is not limiting the reducing equivalent, NADPH, under non-growing conditions:

$$r_1: BuOH + NADP^+ \rightarrow But + NADPH + H^+ \quad (4)$$

$$r_2: But + O_2 + NADPH + H^+ \rightarrow MePr + H_2O + NADP^+ \quad (5)$$

$$r_3: But + O_2 + NADPH + H^+ \rightarrow EtAc + H_2O + NADP^+ \quad (6)$$

The catabolism of glucose required for cell maintenance was modeled as:

$$r_4: C_6H_{12}O_6 + 6\,O_2 \rightarrow 6\,CO_2 + 6\,H_2O \quad (7)$$

The material balance for each component in the liquid phase was:

$$\frac{dn_{BuOH,L}}{dt} = -\theta_{BuOH} - r_1 \times V_L \quad (8)$$

$$\frac{dn_{But,L}}{dt} = r_1 \times V_L - \theta_{But} - (r_2 + r_3) \times V_L \quad (9)$$

$$\frac{dn_{MePr,L}}{dt} = r_2 \times V_L - \theta_{MePr} \quad (10)$$

$$\frac{dn_{EtAc,L}}{dt} = r_3 \times V_L - \theta_{EtAc} \quad (11)$$

$$\frac{dn_{wat,L}}{dt} = (r_2 + r_3 + 6\,r_4) \times V_L - \theta_{wat} \quad (12)$$

$$\frac{dn_{O,L}}{dt} = -\theta_O - 6\,r_4 \times V_L - (r_2 + r_3) \times V_L \quad (13)$$

$$\frac{dn_{C,L}}{dt} = 6\, r_4 \times V_L - \theta_C \qquad (14)$$

The formation rates of the enzymatic reactions, r, depend on the concentration of limiting substrate in the media, according to (Briggs and Haldane, 1925):

$$r = r_{max} \times \frac{C_i}{K_{M_i} + C_i} \qquad (15)$$

It is clear from eq. 15 that the rate of product formation resembles a zero-order reaction when the substrate concentration saturates the enzyme ($r = r_{max}$). When the substrate concentration becomes severely limiting ($K_{M_i} \gg C_i$), however, this resembles a first-order reaction where r is proportional to C_i. The binding affinities (K_{M_i}) for 2-butanol, butanone, oxygen, and NADPH have been previously determined using the non-fused enzymes, with experimental values of 8.63 mM, 381 µM, 18 µM, and 7 µM, respectively (Fraaije et al., unpublished work), and the values have been used as starting point for eq. 15.

For the vapor phase, the material balances consider the molar air inflow (F_{in}) and gas outflow (F_{out}):

$$\frac{dn_{i,G}}{dt} = F_{in} \times y_{i,in} + \theta_i - F_{out} \times y_{i,out} \qquad (16)$$

The air inflow was assumed to contain 20.95% O_2, 0.04% CO_2, and 79.01% N_2. Since N_2 is neither produced nor consumed during the fermentative process, the material

balance considers that $dn_{N,L}/dt = 0$. The pressure in the headspace is constant at 1 bar. The off-gas flow, F_{out}, can be written as a function of the total amount of moles in the headspace of the reactor:

$$F_{out} = F_{in} + \sum \theta_i \quad (17)$$

The transfer rate θ_i of volatile compounds through the vapor/liquid interface relates to the mass transfer coefficient $k_{L,i}a$ and the concentration at the liquid interface $C^*_{i,L}$:

$$\theta_i = k_{L,i}a \times (C_{i,L} - C^*_{i,L}) \times V_L \quad (18)$$

The mass transfer coefficient is strongly dependent on the equipment and medium composition, and once the $k_{L,O_2}a$ value is known within a given system, it can also be determined for the other components in that system based on diffusion coefficient values (Truong and Blackburn, 1984):

$$k_{L,i}a = k_{L,O_2}a \times \frac{D_{i,L}}{D_{O_2,L}} \quad (19)$$

The value of $k_{L,O_2}a$ was determined experimentally using the dynamic method (Tribe et al., 1995). The Wilke–Chang estimation method was used to determine the diffusion coefficients of O_2 and CO_2 in water, while the Tyn–Calus method was applied to estimate the diffusion coefficients of 2-butanol, butanone, ethyl acetate and methyl propionate (Poling et al., 2000). The stripping of water is mainly controlled by gas phase mass transfer resistance, and $k_{L,H_2O}a$ was thus determined using the diffusion

coefficient of water vapor in air, according to Lennard-Jones correlation (Poling et al., 2000). $C_{i,L}^{*}$ can be related to the partition coefficient K_i according to:

$$C_{i,L}^{*} = K_i \times y_i \times \frac{\rho_{wat}}{\sum x_i \times M_{w,i}} \quad (20)$$

K_i was predicted using the modified-UNIFAC model along with Raoult's law accounting for non-ideality (Lohmann et al., 2001):

$$K_i = \frac{x_i}{y_i} = \frac{P}{\gamma_i P_i^{Sat}} \quad (21)$$

O_2 and CO_2 transfer through the interface depend on their saturation concentrations on the liquid phase, which were predicted using Henry coefficients:

$$C_{i,L}^{*} = y_i \times \frac{P}{H_i} \quad (22)$$

Using this structured model, the maximum rates of enzymatic reactions, r_{max}, were estimated by non-linear minimization of the sum of squared residuals between model estimates and experimental data, via Matlab R2014b (Mathworks). The experimental feed composition, expressed in terms of molar concentrations, was used as starting point for the simulations. Matlab ODE15s, appropriate for stiff differential equations, iteratively solved the equations 1–22, with t as the independent variable.

2.5.2. Process design for integrated product recovery

Aspen Plus® V8.8 (Aspen Technologies, Inc., USA) was used to simulate the biotransformation integrated with product recovery, aiming at a methyl propionate production capacity of 120 kton/a, operating time of 8000 h/a, and 98% recovery yield. The formation rate of methyl propionate, as determined from the batch biotransformation tests, was used to determine the cell mass requirements for the full-scale operation. The feedstocks considered were 2-butanol and corn stover hydrolysate, containing glucose at 120 g/kg (Humbird et al., 2011). The design procedures followed the guidelines provided by Seider et al. (2008) and Humbird et al. (2011). The NRTL (non-random two-liquid model) model was selected as thermodynamic property method to predict liquid-liquid equilibrium and vapor-liquid equilibrium for non-ideal solutions. It was assumed that the cells were first grown in a continuous seed-fermentor under inducing conditions, and then transferred to the production vessel to make up for cell washout. The metabolic equation for cell growth, based on the elemental and enthalpy balances as proposed by Heijnen and Roels (1981), is:

$$0.258\ C_6H_{12}O_6 + 0.500\ O_2 + \ 0.200\ NH_4^+ \rightarrow CH_{1.8}O_{0.5}N_{0.2} + 0.550\ CO_2 + 0.950\ H_2O + 0.200\ H^+ \quad (23)$$

The production vessel was simulated as an ideally mixed continuous stoichiometric reactor at 24°C and 1 bar. The cells were kept under non-growing conditions using nitrogen limitation, and air was sparged at 1 vvm to avoid oxygen limitation and fulfil both cell maintenance and enzymatic conversion requirements. The broth concentrations of 2-butanol, butanone, and oxygen were defined based on their binding affinities (K_{M_i}). Product recovery and purification was performed by means of vapor compression,

followed by distillation and decantation. Impurities resulting from cell metabolism and lignocellulose hydrolysis are mostly nonvolatile, and were thus considered to be purged along with the process wastewater. Volatile impurities recoverable by distillation (e.g. furans) were not considered in the present study for the sake of simplification.

The overall economic potential was evaluated using an economic black box model, where governing factors such as annual raw materials and utility costs were considered, while the capital costs were neglected. Recalling the CHMO selectivity for the isomers, 159 kton/a ethyl acetate is additionally produced. The price of petrochemical methyl propionate and ethyl acetate has been estimated as 0.91 €/kg and 0.93 €/kg, respectively (Straathof and Bampouli, 2017).

3. Results and Discussion

3.1. Methyl propionate production in shake flasks

Recombinant cells containing the fusion constructs TmCHMO-MiADH and TbADH-TmCHMO revealed analogous growth behavior. Enzyme induction did not affect microbial growth. The highly enriched TB led to faster microbial growth, $\mu_{max} =$ 0.48±0.04 h^{-1}, as opposed to 0.27±0.02 h^{-1} in MM. Although full glucose consumption has been observed in MM, the low cell density achieved (0.98±0.03 g/L) suggests that part of the energy source is used for maintenance and other non-growth related requirements. In TB, glycerol was fully depleted but the yeast extract could not be quantified. Cell density in this medium reached 2.41±0.11 g/L.

SDS-PAGE analysis confirmed that enzyme expression was poor in MM when compared to TB, and the target enzymes were mostly obtained in an insoluble form, probably aggregated within inclusion bodies (Rosano and Ceccarelli, 2014). Still,

TmCHMO-MiADH enzymes exhibited higher activity in both media, particularly in TB, where full substrate conversion was achieved 24 h after induction. The maximum concentrations of ethyl acetate and methyl propionate in the aqueous broth reached 349±1 mg/L and 206±1 mg/L, respectively, with a regioselectivity of 38±4% towards methyl propionate. Product loss due to the vented cap could not be entirely prevented, and it was estimated as 41.8±0.4 mol%. This value is in fair agreement with what was predicted using the UNIFAC model (38±5 mol%).

3.2. Process integration with *in-situ* gas stripping and absorption by a liquid solvent

The gas stripping of 2-butanol, butanone, methyl propionate and ethyl acetate was examined abiotically using model solutions. The extent of product recovery was studied using air flows of 1.0 and 2.5 vvm, corresponding to $k_{L,O_2}a$ of 25 and 75 h^{-1}, respectively. The average of the results from duplicate tests is shown in Fig. 3 A. The high volatility of butanone, ethyl acetate and methyl propionate, with respective vapor pressures of 0.115 bar, 0.120 bar, and 0.109 bar at 24 °C, boosted mass transfer to the vapor phase, facilitating product evaporation: without an auxiliary absorbent, less than 5 wt.% was recovered by condensation.

To promote the laboratory-scale recovery of volatiles, absorbents were pre-screened among available esters, ketones, alcohols and ethers, using the methodology proposed by Gmehling and Schedemann (2014). The distribution coefficient (recall eq. 21) and selectivity ($\alpha_{MePr/wat} = K_{MePr}/K_{wat}$) of organic solvents for methyl propionate absorption from a representative vapor mixture were predicted. Because of its ready availability, low volatility (T_b =126 °C), fairly high distribution coefficient (8.7) and

selectivity (4.0) for methyl propionate, butyl acetate was used as absorbent in this study. Yet, full recovery could not be achieved (see Fig. 3B). Although 2-butanol could be fully condensed given its lower vapor pressure at the operational temperature (0.022 bar), great losses were observed for the other compounds. This shows the need for compressing the off-gas and cooling it below the dew point of the mixture.

The mathematical model could describe the abiotic gas stripping process with a high coefficient of determination (Fig. 3A, $R^2 = 0.998$). Despite the slightly overestimated stripping rate of 2-butanol, the results suggest that the model is useful to quantify the stripping rates in the presence of product formation.

Biotransformations were performed using the cells containing TmCHMO-MiADH in both MM and TB media. As observed in shake flask experiments, the microbial growth was hindered in MM, and the dry cell concentration did not exceed 5.9±0.1 g/L, even when yeast extract was added to promote growth. Maintenance requirements for these *E. coli* cells (recall r_4) were estimated to be 0.0052 mol_S/(L h). When the biotransformation was terminated, the maximum butanone concentration in the media was 77.35±0.05 mg/L, and no esters were produced, suggesting that the CHMO activity was inhibited in the presence of glucose. This expression pattern is expected when the genes are under control of the arabinose promoter P_{BAD}. Therefore, P_{BAD} may not be suitable to express the genes of interest in this case, as the substrate for this process is lignocellulosic.

When the biotransformation was performed using TB media, during exponential cell growth only 2-butanone accumulated in the media without any ester formation. However, when the cells achieved stationary phase roughly 15 h later, 2-butanol was again added. Fig. 4 shows that the cascade conversion of 2-butanol into butanone, and

butanone into the esters, was immediate, suggesting that the ADH is catalytically active during exponential growth, but the CHMO only becomes active during the stationary phase. This observation might be related to the unavailability of NADPH for the CHMO during microbial growth (Julsing et al., 2012; Walton and Stewart, 2002).

This exemplary biotransformation demonstrates the effectiveness of the model, represented by the lines in Fig. 4 (R^2 = 0.988), using as fitting parameters $r_{1,max}$ = 1.14±0.36 g_{But}/(L h), $r_{2,max}$ = 0.09±0.02 g_{MePr}/(L h), and $r_{3,max}$ = 0.11±0.01 g_{EtAc}/(L h). The formation rates of esters indicated an actual regioselectivity of 43±9% for the ester of interest, methyl propionate. The studies revealed that MiADH is converting 2-butanol into butanone 5.7-fold faster than TmCHMO is converting butanone into esters and, as a result, full saturation of the CHMO occurred for the range of concentrations tested. These values were used to assess the performance of the full-scale biotransformation integrated with product recovery and purification.

3.3. Prospects for the biotransformation integrated with product recovery

A preliminary analysis was performed to assess the cell mass and feedstock needs for the proposed process, including seed fermentors and maintenance costs. Bioreactors of 500 m^3, with 70% working volume and maximum cell concentration of 50 g/L were considered. The results, shown in Table 1, uphold previous studies stating that volume-specific productivities below 2 g/(L h) are uncommercializable (Van Dien, 2013). Given the discrepancy between the reaction rates of MiADH and TmCHMO, a significant fraction of the produced butanone either accumulates in the media or is stripped along with the vapor phase (>70 wt.%). To achieve the required ester productivity, more than 104.5 ton_{BuOH}/h are used, and the fermentation feedstock costs rise to ca. 944 million

€/a. Also, due to the azeotropes that are formed between butanone, 2-butanol, water, and the esters, separation by conventional distillation becomes impracticable, anticipating severe operational costs. Ideally, the accumulation of butanone should be minimized while still allowing for full enzyme saturation. Hence, a different scenario was investigated where the observed MiADH productivity was used, and the TmCHMO productivity was tuned accordingly. As a result, the TmCHMO productivity used for design was ~7-fold the experimental, leading to accordingly decreased cell mass, broth volume, and hydrolysate requirements (see Table 1). Under these conditions, the efficiency of product recovery becomes the major focus for the profitability of the overall process. Therefore, product recovery costs have been estimated.

A flow diagram illustrating the integrated conceptual process is shown in Fig. 5, and the operational conditions used in the distillation units are depicted in Table 2. The aqueous broth containing ca. 8.5 g_{MePr}/L and 13.2 g_{EtAc}/L, concentrations below inhibiting threshold levels (Pereira et al., 2016), was first centrifuged for cell mass separation and recycle (98.5 wt.%), and then distilled for water removal (D1). The enriched vapor, comprising 88 wt.% of the volatile biotransformation products, is compressed for inert gas removal. In this step, 99 wt.% of the vapor products are lost at room temperature and pressure, which was minimized to 2 wt.% using compression to 30 bar with cooling to 2°C. The condensate was mixed with the distillate from D1 in a decanter, and the solubility properties of the resulting mixture enabled the concentration of esters in the organic phase beyond azeotropic compositions, facilitating further separation by distillation.

2-Butanol was first separated from the esters in D2, and the resulting stream, containing ca. 7.9 g_{EtAc}/L and 46.4 g_{MePr}/L, was recycled back to the production vessel. Due to a

small relative volatility (1.077), methyl propionate and ethyl acetate can only be separated at the expense of extremely large distillation columns (D3). Under the current conditions, the distillate contained mainly ethyl acetate (85 wt.%), which was not purified further, while the bottom stream comprises the purified methyl propionate (99.78 wt.%), containing traces of 2-butanol (0.17 wt.%) and ethyl acetate (0.05 wt.%). Taking into account an assumed 20% penalty in the price of ethyl acetate, given its lower purity, the expected revenue for this process is 235 million €/a. The overall energy duty after heat integration was 1256 GJ/h (34.7 MJ/kg_{ester}). The cooling required for the biotransformation task represents a major energy sink in the process (41% of the total duty), along with the product purification task (41%), and vapor compression (15%). Under the present conditions, the total variable operating costs ascend to 335 million €/a (76% biotransformation; 14% vapor compression; 8% product purification). This translates into 1.16 €/kg_{ester}, which is beyond the petrochemical price of methyl propionate.

By shifting completely the TmCHMO selectivity to methyl propionate, the volume-specific productivity would double, and significant capital and operating savings would be achieved, as the biotransformation costs would decrease by ca. 57%. Additionally, the ester separation task could be avoided, as only 2-butanol would be recovered and recycled to the bioreactor. However, 2-butanol is the main substrate for the enzymatic conversion, with a requirement of 0.84 g/g_{ester}. Taking the bio-based 2-butanol selling price of ca. 0.9 €/kg (Pereira et al., 2017), this represents 93% of the expected process revenues, and 69% of the total variable operating costs. In fact, even in case of full TmCHMO selectivity for methyl propionate, the 2-butanol demand would represent 83% of the product sales revenues. This suggests that the bio-based production of

methyl propionate can only become profitable if the production cost of bio-based 2-butanol is minimized. Using a dilute stream instead of pure 2-butanol would decrease its cost, but water distillation would become a significant expenditure in the present configuration. A biotransformation in which 2-butanol is produced in the same vessel as the esters at an appropriate rate, or a one-step conversion promoting methyl propionate formation directly from glucose, would avoid the need for 2-butanol recovery, and could enhance the maximum yield to 0.489 $g_{ester}/g_{glucose}$. Nevertheless, the microbial metabolic requirements and biotransformation are expected to be extremely demanding.

4. Conclusions

A novel bio-based approach for methyl propionate production has been assessed. Even though the pathway for bio-based methyl propionate has been implemented, significant strain optimization is still required. The enhancement of the activity/selectivity of the CHMO for methyl propionate can lead to significant feedstock and energy savings. Overall, the proposed two-step process appears to be suboptimal for microbial ester production due to substrate, product, and energy losses. This study suggests that avoiding 2-butanol recovery is crucial to achieve a profitable process, and a one-step microbial process for simultaneous 2-butanol and ester production should be aimed at.

Acknowledgments

The authors thank Prof. Dr. Marco Fraaije and Dr. Elvira Guzman, from the Molecular Enzymology Group, Groningen Biomolecular Sciences and Biotechnology Institute, for kindly providing the recombinant cells. Rosario Medici, Maria Cuellar, Bhargavi

Ganesan, Yi Song, Max Zomerdijk, Stef van Hateren, and Linda Otten are to be acknowledged for their analytical support and fruitful advice.

Conflict of interest

The authors declare no commercial or financial conflict of interest.

Funding

This work was supported by The Netherlands Organization for Scientific Research (NWO) under the framework of Technology Area TA-Biomass.

Nomenclature

C	mol/L	Concentration
C^*	mol/L	Concentration at the liquid interface
D	cm^2/s	Diffusivity
F	mol/h	Mole flow rate
H	bar/(mol L)	Henry coefficient
$k_L a$	1/h	Volume-specific mass transfer coefficient
K_i	bar/bar	Distribution coefficient
K_M	mol/L	Michaelis constant
M_w	g/mol	Molecular mass
n	mol	Number of moles
P	bar	Pressure
P^{Sat}	bar	Saturation pressure
r	mol/(L h)	Rate of formation

t	h	Time
T	K	Temperature
V	L	Volume
x	–	Mole fraction in the liquid phase
y	–	Mole fraction in the vapor phase
Greek Symbols		
γ	–	Activity coefficient
μ	1/h	Microbial growth rate
θ	mol/h	Transfer rate from liquid to gas phase
ρ	g/L	Density
Subscripts		
$BuOH$		2-Butanol
But		Butanone
C		Carbon dioxide
$ester$		Ester (methyl propionate or ethyl acetate)
$EtAc$		Ethyl acetate
G		Gas phase
i		Component i
j		Component j
L		Liquid phase
max		Maximum rate
$MePr$		Methyl propionate
N		Nitrogen

O	Oxygen
S	Substrate
sol	Organic solvent
X	Cell mass

References

1. Aalbers, F.S., Fraaije, M.W. 2017. Coupled reactions by coupled enzymes: alcohol to lactone cascade with alcohol dehydrogenase-cyclohexanone monooxygenase fusions. Appl. Microbiol. Biotechnol., 101(20), 7557–7565.

2. Ali, U., Karim, K.J.B.A., Buang, N.A. 2015. A Review of the Properties and Applications of Poly (Methyl Methacrylate) (PMMA). Polym. Rev., 55(4), 678–705.

3. Briggs, G.E., Haldane, J.B.S. 1925. A Note on the Kinetics of Enzyme Action. Biochem. J., 19(2), 338–339.

4. Chen, Z., Sun, H., Huang, J., Wu, Y., Liu, D. 2015. Metabolic Engineering of Klebsiella pneumoniae for the Production of 2-Butanone from Glucose. PLOS ONE, 10(10), e0140508.

5. Clegg, W., R. J. Elsegood, M., R. Eastham, G., P. Tooze, R., Lan Wang, X., Whiston, K. 1999. Highly active and selective catalysts for the production of methyl propanoate via the methoxycarbonylation of ethene. Chem. Commun.(18), 1877–1878.

6. de Vrije, T., Budde, M., van der Wal, H., Claassen, P.A.M., López-Contreras, A.M. 2013. "*In situ*" removal of isopropanol, butanol and ethanol from fermentation broth by gas stripping. Bioresour. Technol., 137(0), 153–159.

7. Eastham, G.R., Johnson, D.W., Straathof, A.J.J., Fraaije, M.W., Winter, R.T. 2015. Process for the production of methyl methacrylate.

8. Global Market Insights, I. 2016. Synthetic and Bio-based PMMA (Polymethyl Methacrylate) Market Size By Product (Extruded Sheets, Pellets, Beads, Cell Cast Sheet & Blocks), By Application (Automotive, Electronics, Construction, Signs & Display), Industry Analysis Report, Regional Outlook, Downstream Application Development Potential, Price Trend, Competitive Market Share & Forecast, 2012-2022.

9. Gmehling, J., Schedemann, A. 2014. Selection of Solvents or Solvent Mixtures for Liquid–Liquid Extraction Using Predictive Thermodynamic Models or Access to the Dortmund Data Bank. Ind. Eng. Chem. Res., 53(45), 17794–17805.

10. Heijnen, J.J., Roels, J.A. 1981. A macroscopic model describing yield and maintenance relationships in aerobic fermentation processes. Biotechnol. Bioeng., 23(4), 739–763.

11. Humbird, D., Davis, R., Tao, L., Kinchin, C., Hsu, D., Aden, A., Schoen, P., Lukas, J., et al. 2011. Process design and economics for biochemical conversion of lignocellulosic biomass to ethanol - Dilute-acid pretreatment and enzymatic hydrolysis of corn stover. NREL - National Renewable Energy Laboratory.

12. Julsing, M.K., Kuhn, D., Schmid, A., Bühler, B. 2012. Resting cells of recombinant E. coli show high epoxidation yields on energy source and high sensitivity to product inhibition. Biotechnol. Bioeng., 109(5), 1109–1119.

13. Kruis, A.J., Levisson, M., Mars, A.E., van der Ploeg, M., Garcés Daza, F., Ellena, V., Kengen, S.W.M., van der Oost, J., et al. 2017. Ethyl acetate production by the elusive alcohol acetyltransferase from yeast. Metab. Eng., 41, 92–101.

14. Liu, J., Heaton, B.T., Iggo, J.A., Whyman, R., Bickley, J.F., Steiner, A. 2006. The mechanism of the hydroalkoxycarbonylation of ethene and alkene-CO copolymerization catalyzed by Pd(II)-diphosphine cations. Chemistry, 12(16), 4417–4430.

15. Lohmann, J., Joh, R., Gmehling, J. 2001. From UNIFAC to Modified UNIFAC (Dortmund). Ind. Eng. Chem. Res., 40(3), 957–964.

16. Löser, C., Schröder, A., Deponte, S., Bley, T. 2005. Balancing the Ethanol Formation in Continuous Bioreactors with Ethanol Stripping. Eng. Life Sci., 5(4), 325–332.

17. Löser, C., Urit, T., Bley, T. 2014. Perspectives for the biotechnological production of ethyl acetate by yeasts. Appl. Microbiol. Biotechnol., 98(12), 5397–5415.

18. Pereira, J.P.C., Lopez-Gomez, G., Reyes, N.G., van der Wielen, L.A.M., Straathof, A.J.J. 2017. Prospects and challenges for the recovery of 2-butanol produced by vacuum fermentation - a techno-economic analysis. Biotechnol. J., 12(7), 1600657.

19. Pereira, J.P.C., Verheijen, P.J.T., Straathof, A.J.J. 2016. Growth inhibition of S. cerevisiae, B. subtilis, and E. coli by lignocellulosic and fermentation products. Appl. Microbiol. Biotechnol., 100, 9069–9080.

20. Poling, B., Prausnitz, J., Connell, J.O. 2000. The Properties of Gases and Liquids. McGraw-Hill Education.
21. Rosano, G.L., Ceccarelli, E.A. 2014. Recombinant protein expression in Escherichia coli: advances and challenges. Front. Microbiol., 5, 172.
22. Seider, W.D., Seader, J.D., Lewin, D.R. 2008. Product and Process Design Principles: Synthesis, Analysis and Design. 3rd Edition ed. Wiley Global Education.
23. Straathof, A.J.J., Bampouli, A. 2017. Potential of commodity chemicals to become bio-based according to maximum yields and petrochemical prices. Biofuels, Bioprod. Biorefin., 11(5), 798–810
24. Tribe, L.A., Briens, C.L., Margaritis, A. 1995. Determination of the volumetric mass transfer coefficient (k(L)a) using the dynamic "gas out-gas in" method: Analysis of errors caused by dissolved oxygen probes. Biotechnol. Bioeng., 46(4), 388–392.
25. Truong, K.N., Blackburn, J.W. 1984. The stripping of organic chemicals in biological treatment processes. Environ .Prog., 3(3), 143–152.
26. Urit, T., Li, M., Bley, T., Löser, C. 2013. Growth of Kluyveromyces marxianus and formation of ethyl acetate depending on temperature. Appl. Microbiol. Biotechnol., 97(24), 10359–10371.
27. Urit, T., Löser, C., Wunderlich, M., Bley, T. 2011. Formation of ethyl acetate by *Kluyveromyces marxianus* on whey: studies of the ester stripping. Bioprocess Biosyst. Eng., 34(5), 547–559.
28. van Beek, H.L., Romero, E., Fraaije, M.W. 2017. Engineering Cyclohexanone Monooxygenase for the Production of Methyl Propanoate. ACS Chem. Biol., 12(1), 291–299.
29. Van Dien, S. 2013. From the first drop to the first truckload: commercialization of microbial processes for renewable chemicals. Curr. Opin. Biotechnol., 24(6), 1061–1068.
30. Walton, A.Z., Stewart, J.D. 2002. An efficient enzymatic Baeyer-Villiger oxidation by engineered Escherichia coli cells under non-growing conditions. Biotechnol. Progr., 18(2), 262–268.
31. Xue, C., Zhao, J., Liu, F., Lu, C., Yang, S.-T., Bai, F.-W. 2013. Two-stage in situ gas stripping for enhanced butanol fermentation and energy-saving product recovery. Bioresour. Technol., 135(0), 396–402.

32. Yoneda, H., Tantillo, D.J., Atsumi, S. 2014. Biological production of 2-butanone in *Escherichia coli*. ChemSusChem, 7(1), 92–95.

Figure Captions

Fig.1. Pathway for the production of methyl methacrylate from lignocellulose via 2-butanol and methyl propionate

Fig. 2. Schematic diagram of the experimental set-up for biotransformation integrated with *in-situ* product recovery by gas stripping and absorption

Fig. 3. (A) Comparison between experimental (markers) and predicted (lines) concentrations of products in the aqueous phase during stripping of model solutions using flow rates of 1.0 vvm (solid lines, full markers) and 2.5 vvm (dash lines, open markers); **(B)** Yield of product recovery in the condensation system achieved in stripping tests with air flow rates of 1.0 vvm (light color) and 2.5 vvm (dark color)

Fig. 4. Aerobic biotransformation using *E.coli* TmCHMO-MiADH in TB medium, comparison between experimental (markers) and predicted (lines) concentrations in the aqueous phase; cell concentration = 7.1±0.8 g/L

Fig. 5. Process flow diagram for ester production using biotransformation integrated with product recovery and purification; C – centrifuge; FT – flash tank; D1/D2/D3 – distillation units

Tables and Figures

Table 1. Requirements for the annual production of 120 kton methyl propionate, using the experimental ADH/CHMO productivity, and a tuned (design) CHMO productivity

	Experimental		Tuned	
	CHMO	ADH	CHMO	ADH
Cell-mass specific productivity (kg/(kg$_X$ h))	0.012	0.158	0.082	0.158
Volume-specific productivity (kg/(m^3 h))	0.597	7.917	4.118	7.917
Volume broth required (m^3)	25629		3717	
Cell mass requirement (ton/a)	1281		186	
2-Butanol requirement (kton/a)	837		244	
Hydrolysate requirement (kton/a)	11094		1609	
Feedstock cost* (M €/a)	944		245	

*considering hydrolysate and 2-butanol

Table 2. Operational conditions in the distillation columns as defined by process design. See Fig. 5 for D1–D3.

Distillation column	D1	D2	D3
Condenser *P* (bar)	1	1	1
Stages (minimum)	2	11	154
Stages (actual)	7	32	285
Feed stage	4	6	80
Reflux ratio	0.33	0.35	27.0
Distillate/feed ratio	0.03	0.99	0.67
T_{bottom} (ºC)	99.6	97.9	79.09
T_{top} (ºC)	94.8	72.2	68.05

Figure 1.

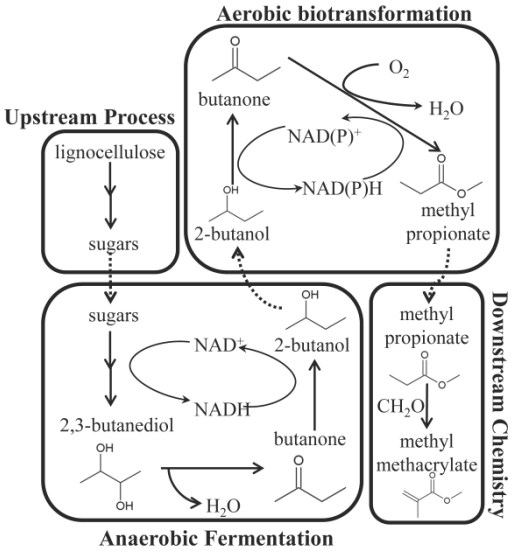
Aerobic biotransformation
butanone
O_2
H_2O
NAD(P)$^+$
NAD(P)H
2-butanol
methyl propionate
Upstream Process
lignocellulose
sugars
sugars
NAD$^+$
NADH
2,3-butanediol
2-butanol
butanone
H_2O
Anaerobic Fermentation
methyl propionate
CH_2O
methyl methacrylate
Downstream Chemistry

Figure 2.

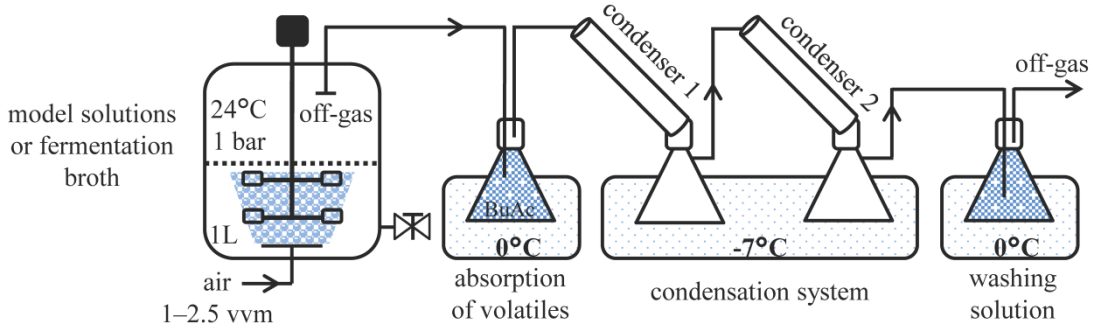
model solutions
or fermentation
broth
24°C
1 bar
off-gas
1L
air
1–2.5 vvm
BuAc
0°C
absorption
of volatiles
condenser 1
condenser 2
-7°C
condensation system
off-gas
0°C
washing
solution

Figure 3. A) B)

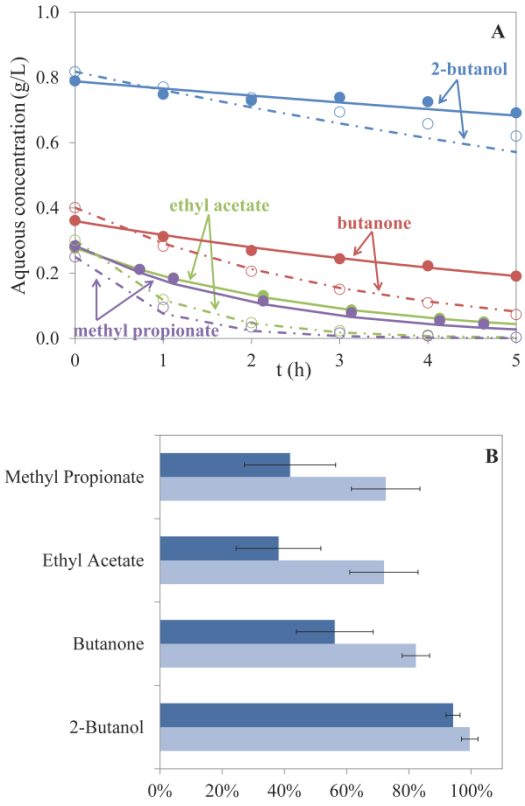
A
2-butanol
ethyl acetate
butanone
methyl propionate
Aqueous concentration (g/L)
t (h)
1.0
0.8
0.6
0.4
0.2
0.0
0
1
2
3
4
5
B
Methyl Propionate
Ethyl Acetate
Butanone
2-Butanol
0%
20%
40%
60%
80%
100%

Figure 4.

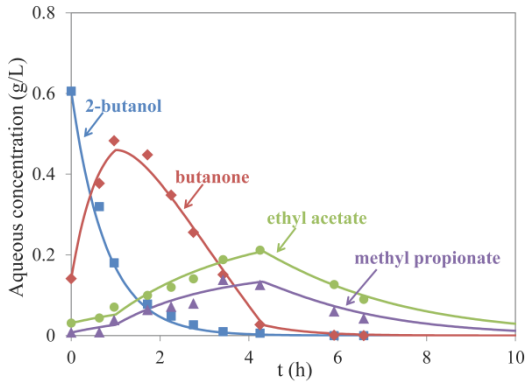
0.8
0.6
0.4
0.2
0
Aqueous concentration (g/L)
2-butanol
butanone
ethyl acetate
methyl propionate
0
2
4
6
8
10
t (h)

Figure 5.

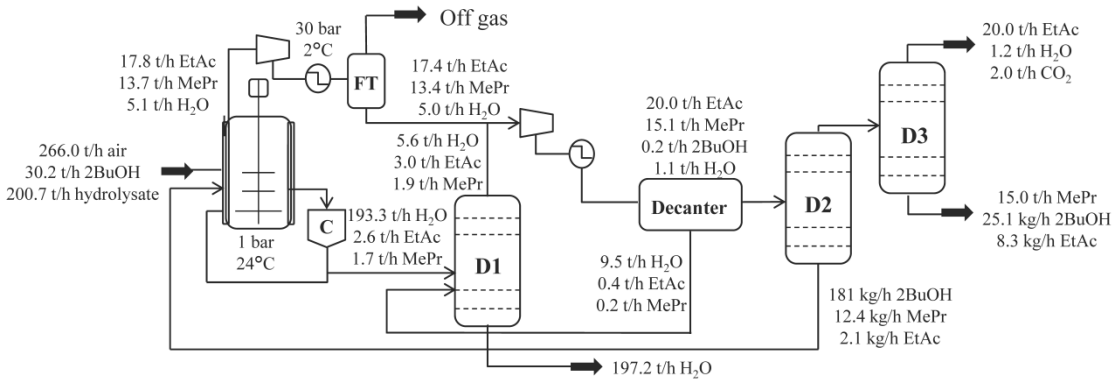
30 bar
2°C
Off gas
17.8 t/h EtAc
13.7 t/h MePr
5.1 t/h H2O
FT
17.4 t/h EtAc
13.4 t/h MePr
5.0 t/h H2O
20.0 t/h EtAc
1.2 t/h H2O
2.0 t/h CO2
D3
266.0 t/h air
30.2 t/h 2BuOH
200.7 t/h hydrolysate
5.6 t/h H2O
3.0 t/h EtAc
1.9 t/h MePr
20.0 t/h EtAc
15.1 t/h MePr
0.2 t/h 2BuOH
1.1 t/h H2O
Decanter
D2
15.0 t/h MePr
25.1 kg/h 2BuOH
8.3 kg/h EtAc
C
193.3 t/h H2O
2.6 t/h EtAc
1.7 t/h MePr
1 bar
24°C
D1
9.5 t/h H2O
0.4 t/h EtAc
0.2 t/h MePr
181 kg/h 2BuOH
12.4 kg/h MePr
2.1 kg/h EtAc
197.2 t/h H2O